Modelling cetacean morbillivirus outbreaks in an endangered killer whale population

Michael N. Weiss[1,2]*, Daniel W. Franks[3], Kenneth C. Balcomb[2], David K. Ellifrit[2], Matthew J. Silk[4], Michael A. Cant[4], and Darren P. Croft[1]

[1] Centre for Research in Animal Behaviour, University of Exeter, Exeter, U.K. EX4 4QG

[2] Center for Whale Research, Friday Harbor, WA, U.S.A. 98250

[3] Department of Biology and Department of Computer Science, University of York, York, U.K. YO10 5DD

[4]Centre for Ecology and Conservation, University of Exeter in Cornwall, Penryn, U.K. TR10 9FE

*Corresponding author

Email: mw607@exeter.ac.uk

Acknowledgements

We would like to thank all of the many volunteers and staff that have contributed to the field work for Orca Survey that provided the photographs used in this study, as well the photographic ID catalogue for this population. We'd also like to thank Emma Foster for her work developing the network construction protocol used here.

Role of funding source

Data collection for this research was supported by funding from Earthwatch Institute and NOAA Fisheries.

Declaration of Interest

The authors declare they have no conflict of interest.

Abstract

The emergence of novel diseases represents a major hurdle for the recovery of endangered populations, and in some cases may even present the threat of extinction. In recent years, epizootics of infectious diseases have emerged as a major threat to marine mammal populations, particularly group-living odontocetes. However, little research has explored the potential consequences of novel pathogens in endangered cetacean populations. Here, we present the first study predicting the spread of infectious disease over the social network of an entire free-ranging cetacean population, the southern resident killer whale community (SRKW). Utilizing 5 years of detailed data on close contacts between individuals, we build a fine-scale social network describing potential transmission pathways in this population. We then simulate the spread of cetacean morbillivirus (CeMV) over this network. Our analysis suggests that the SRKW population is highly vulnerable to CeMV. The majority of simulations resulted in unusual mortality events (UMEs), with mortality rates predicted to be at least twice the recorded maximum annual mortality. We find only limited evidence that this population's social structure inhibits disease spread. Vaccination is not likely to be an efficient strategy for reducing the likelihood of UMEs, with over 40 vaccinated individuals (>50% of the population) required to reduce the likelihood of UMEs below 5%. This analysis highlights the importance of modelling efforts in designing strategies to mitigate disease, and suggests that populations with strong social preferences and distinct social units may still be highly vulnerable to disease outbreaks.

Keywords: social network, epidemic modelling, *Orcinus orca*, SRKW, vaccination

Introduction

Infectious diseases, particularly novel pathogens emerging in naïve populations, can have severe consequences for animal populations (Daszack *et al.* 2000). The consequences of these pathogens are exacerbated in small, endangered populations, where disease can contribute to elevated extinction risk (Pedersen *et al.* 2007). The prediction of infectious disease outbreaks through epidemic modelling, and the subsequent design of mitigation strategies, is therefore a key task in endangered species management. Traditional epidemic models assume that contact rates are homogenous within a population (Allen 2008). However, this is rarely the case. In populations that are strongly spatially or socially structured, these assumptions may hamper efforts to predict the severity and patterning of disease outbreaks.

Network-based models have been increasingly used for analyzing disease dynamics in animal populations, because they can incorporate spatial and social structure (Craft & Caillaud 2011; Godfrey 2013; Silk *et al.* 2017). In social network models, social entities (i.e. individuals or groups) are represented as nodes in a graph, with the edges between nodes representing social connections and thus the opportunity for disease transmission. A great deal of research has modelled disease outbreaks over the social networks of terrestrial mammal populations, with the goals of predicting outbreak sizes, estimating temporal trends in susceptibility, and designing vaccination strategies (e.g. chimpanzees (*Pan troglodytes*) and orangutans (*Pongo pygmaeus*): Carne *et al.* 2014; raccoons (*Procyon lotor*): Reynolds *et al.* 2015; Japanese macaque (*Macaca fuscata*): Romano *et al.* 2016; chimpanzees: Rushmore *et al.* 2014; African buffalo (*Syncerus caffer*): Cross *et al.* 2004; Verreaux's sifakas (*Propithecus verreaxi*): Springer *et al.* 2017; European badgers (*Meles meles*): Rozins & Silk *et al.* 2018). This work has highlighted the importance of considering non-random social structures in wildlife epidemic modelling, and has suggested a role for social structure in containing epidemics in natural populations.

Emergent infectious disease is of increasing concern for populations of cetaceans, many of which are already threatened or endangered (Gulland & Hall 2007; Van Bressem *et al.* 2009). Relatively little work, however, has been done modelling the disease consequences of cetacean social structure. Guiamares *et al.* (2007) modelled the spread of a hypothetical pathogen in a subnetwork of mammal eating killer whales (*Orcinus orca*), finding that the network was particularly vulnerable to disease outbreak. In this analysis, the dynamics of the simulation were not tuned to any particular pathogen. More recently, unweighted versions of networks derived from bottlenose dolphin populations (*Tursiops truncatus*) have been analyzed as part of comparative and theoretical studies (Sah *et al.* 2017; Sah *et al.* 2018). Importantly, no

previous study has modelled the spread of specific pathogens over cetacean social networks with the goal of predicting the severity of outbreaks, and none have modelled the spread through a complete population.

Due to the logistical challenges of observing social interactions in wild cetaceans, the vast majority of cetacean social network studies are based on association indices, which estimate the probability that dyads associate in a given sampling period. Criteria for "association" are varied, but researchers typically set a temporal or spatial threshold at which two individuals are considered to be together. A mismatch between association criteria and disease transmission scales may have hampered previous epidemiological studies; most cetacean social network studies that use a spatial threshold define associations on broad scales, from 100 m (e.g. Lusseau *et al.* 2006) up to 10 km (e.g. Foster *et al.* 2012). While these association criteria are often justified when trying to understand the patterns of social relationships within a population, many pathogens of interest are typically transmitted over smaller spatial scales, e.g. when animals exchange viruses through the respiratory tract. This mismatch between contacts relevant to infection and network definitions may lead to incorrect inferences about the dynamics of disease outbreaks (Craft 2015).

A pathogen of particular concern in gregarious cetacean species is cetacean morbillivirus (CeMV). CeMV is an RNA virus belonging to the family *Paramyxoviridae*, which also contains measles virus, phocine distemper virus, canine distemper virus, feline morbillivirus, and peste des petits ruminants virus (Alfonso *et al.* 2016). CeMV is implicated as the cause of several unusual mortality events in wild cetaceans (Van Bressem *et al.* 1999; Di Guardo *et al.* 2005). This virus is highly infectious, with high potential for interspecies transmission (Jo *et al.* 2018) and is likely transmitted via the respiratory tract through the inhalation of aerosolized virus (Van Bressem *et al.* 2014). Several factors may increase a population's susceptibility to CeMV, including high polychlorinated biphenyl (PCB) load (Aguilar & Borrell 1994), poor nutrition (Aguilar & Raga 1993) and inbreeding (Valsecchi *et al.* 2003).

In this study, we use detailed social network data to model disease dynamics in an endangered killer whale population, the southern resident killer whales (SRKW). The SRKW population is an extremely small (less than 80 individuals), closed population of killer whales in the northeastern Pacific, frequenting the inland waters of Washington and British Columbia. This population faces long-term threats from a variety of environmental and anthropogenic factors. The three factors identified as primary hazards to this population are the decline in abundance and quality of their primary prey, Chinook salmon (*Oncorhynchus tshawytscha*), anthropogenic noise, and persistent organic pollutants (Lacy *et al.* 2017). In addition, recent

analysis of the respiratory microbiome of this population has highlighted pathogens as a potential fourth threat (Raverty *et al.* 2017). Previous analysis has emphasized CeMV as a pathogen in need of further study and monitoring in this population (Gaydos *et al.* 2004).

Killer whales are susceptible to CeMV infection; an Atlantic killer whale that stranded in 2002 was found to be seropositive for CeMV antibodies, indicating recent exposure (Rowles *et al.* 2011). Morbillivirus epizootics have not yet been recorded in any killer whale population and the virus has not been detected in Pacific killer whales, but CeMV has high spillover potential from reservoirs into novel populations (Van Bressem *et al.* 2014). SRKWs have been observed interacting with other cetacean species which are known carriers of CeMV, including harbor porpoise (*Phocoena phocoena*), humpback whales (*Megaptera novaengliae*), and Pacific white-sided dolphins (*Lagenorhynchus obliquidens*), providing a potential pathway for the introduction of this pathogen into the population. In addition, many of the factors that are thought to increase a population's susceptibility to CeMV are present in the SRKW community, including high PCB load, inbreeding, and nutritional stress (Krahn *et al.* 2007; Ford *et al.* 2018; Ford *et al.* 2010).

The SRKW live in stable, multilevel social groups, and individuals form distinct social clusters (Bigg et al. 1990; Parsons *et al.* 2009; Ellis *et al.* 2017). The smallest, most stable social unit is the matriline, composed of females and their descendants, which usually contain 2-9 whales. Closely related matrilines form pods that may contain over 40 individuals and exhibit distinct vocal dialects. The southern resident community contains 3 pods, referred to as J, K, and L (Bigg *et al.* 1990). This social organization creates a modular social network structure, although the implications of this multilevel social structure for disease transmission in this population has yet to be established.

Modular networks have been hypothesized to provide fitness benefits to social species by trapping disease within modules and preventing large-scale epidemics. Simulation studies predict that modular contact networks result in smaller disease outbreaks than non-modular networks (Nunn *et al.* 2015; Sah *et al.* 2017; Rozins & Silk *et al.* 2018). Recent comparative work has suggested that network subgrouping may decrease outbreak size and epidemic probability, dependent on the characteristics of the disease and strength of the subdivisions (Sah *et al.* 2018). An analysis of parasite load in primate social groups supports the hypothesis that modular organization inhibits disease spread, with individuals in more modular groups generally having lower parasite load (Griffin & Nunn 2012). In addition, the presence of pronounced social preferences may itself aid in preventing disease spread. Strong social preferences result in increased variance in edge weights (Whitehead 2008), and social networks with greater variance in edge weight are

predicted to generally experience smaller outbreaks of infectious disease (Yang & Zhou 2012; Wang *et al.* 2014). It is currently unclear if the modular structure and strong social preferences of the SRKW community are capable of significantly reducing disease spread. Previous work in a closely related species with a similar social structure, the long-finned pilot whale (*Globicephala melas*), demonstrated that increased mortality after a CeMV epizootic was limited to a subset of social groups (Wierucka *et al.* 2014), potentially indicating that modular social structures can effectively trap this disease.

Recently, there has been growing interest in applying individualized medical treatment to the SRKW population (e.g. NOAA 2018), following the model of wildlife veterinary care that has been applied in terrestrial systems such as mountain gorillas (Robbins *et al.* 2011). Such individualized care may include prophylactic vaccination strategies. Although no morbillivirus vaccine is proven to be effective in any cetacean species, a DNA vaccine for CeMV has been tested in bottlenose dolphins (Vaughan *et al.* 2007) and recent genomic studies could further inform the development of new vaccines (Batley *et al.* 2018). Logistical challenges and ethical considerations, however, may preclude vaccinations on a large scale in wild populations. Nonetheless, network-based vaccination strategies to mitigate morbillivirus spread have been successfully implemented in another endangered marine mammal, the Hawaiian monk seal (*Monachus schauinslandi*; Robinson *et al.* 2018). Furthermore, herd immunity is thought to be more easily induced in modular social networks, as individuals that bridge communities can be targeted for vaccination, preventing global disease spread (Salathe & Jones 2010). It is currently unclear whether vaccinating a realistic portion of the SRKW population would be effective at preventing epizootics.

Here, we use five years of detailed, fine-scale association data to inform a stochastic, network-based model of pathogen spread through the SRKW population. We focus on simulating the epidemic characteristics of cetacean morbillivirus based on previously published research, given its role in mass mortality in other populations and the risk it poses to the SRKW. We further use null models of the social network to determine the role that social structure has in shaping disease outbreaks. Finally, we simulate both random and network-based vaccination strategies to determine if prophylactic treatment could efficiently mitigate epizootics in this population.

Methods

Field observations

Social associations were recorded over five years (2011-2015) of opportunistic photographic identification surveys in the inland waters of Washington and British Columbia conducted by the Center for Whale Research (CWR). The purpose of these surveys was both to capture clear images of every whale present during each encounter and to acquire photographs that could be used for assessment of body condition and social affiliations. As the SRKW are protected by federal law in both the United States and Canada, all field work was carried out under federal permits issued by both countries (NMFS 15569; DFO SARA 272). Surfacing whales were photographed using Canon or Nikon DSLR cameras. Encounters only occurred on days when clear photographic identification was possible (i.e. no rain and sea state less than Beaufort 4). As the CWR has been conducting annual surveys of the SRKW population since 1976, all individuals in this population are well known. Individuals are easily identifiable throughout their lives by unique pigmentation patterns behind their dorsal fins ("saddle patches"), as well as by dorsal fin shape, knicks, and scars they acquire throughout their lives (Bigg *et al.* 1990). Surveys were typically conducted from small motorized vessels (5.5 m Boston Whaler), although shore-based photographs of sufficient quality to identify individuals and associations were also analyzed. Only in-focus, clear photograph sequences in which all individuals were identifiable were analyzed. Photographs were managed and analyzed using ACDSee Photo Studio.

Social network construction

As CeMV is thought to be contracted primarily through the inhalation of aerosolized virus, our contact network was constructed to reflect close surface associations, with the goal of estimating the frequency of "respiratory contact" between dyads. While much is still unknown about the transmission dynamics of CeMV, including how long the virus remains infectious in the air after exhalation, we chose a restricted association criteria to ensure that our estimates of disease spread were conservative. Therefore, we considered individuals surfacing synchronously or successively within one body length to be in respiratory contact. Synchronous and successive surfacings were recorded from photographic series capturing surfacing sequences. A surfacing was considered successive or synchronous when an individual began surfacing before the previous individual became completely submerged (Figure 1a).

Individuals and social groups within the SRKW population differ in their use of the study area, and were not continuously followed. Therefore, we are unable to directly estimate the total number of contact events between individuals. Instead, we estimate the probability that each dyad came into contact on a

given day. We estimated daily respiratory contact probabilities by calculating dyadic simple ratio indices (SRI; Cairn & Schwager 1987):

$$\mathrm{SRI}_{ij} = \frac{X_{ij}}{D_{ij}} \quad (1)$$

where X_{ij} is the number of days in which individual *i* was photographed in respiratory contact with individual *j*, and D_{ij} is the total number of days on which either *i* or *j* were photographed. SRI values represent an estimated daily association probability, and thus range from 0 to 1, with zero indicating individuals were never observed in respiratory contact, while 1 indicates individuals were observed in respiratory contact on every day that either was observed. Many cetacean network studies use a half-weight index (HWI) to correct for biases in data collection, namely that individuals are often more likely to be seen apart than together. However, in line with our goal of being conservative in our estimates of disease spread, we chose to use SRI, as a dyad's SRI value will always be less than or equal to the same dyad's HWI value.

During surveys, the primary objective was to photograph all whales present, with secondary goals of recording social groupings and assessing the health of individuals. Groups of whales could not be continually followed for all hours of the day, and it was therefore not possible to quantify the amount of time associated dyads spend together on a given day. Moreover, not all individuals could be simultaneously monitored and surveys were likely to miss surface associations. Therefore, our SRI values are prone to underestimating daily contact probabilities, which may lead to overly-conservative estimates of disease outcomes.

We limit our dataset to sampling days occurring in the summer months (May to September) of each year. This is the period in which the southern residents are most frequently in the study area as they follow returning Chinook salmon runs, and therefore provides the most detailed data on association patterns. While some aspects of SRKW social structure change over longer time-scales, relationships are consistently structured by pod and matriline, and changes are not predictable (Parsons *et al.* 2009). Therefore, we aggregate association data across the entire study period, as this aggregation allows for more precise estimates of dyadic contact probabilities (Whitehead 2008). In order to avoid biases in estimated contact probabilities due to the births and deaths of individuals, only individuals that were alive for the entire study period were included in our analysis.

To confirm the suitability of this approach, we compared all pairs of networks derived from each year of data collection by calculating the Spearman correlation coefficient between dyadic SRI values across the

two years, with Mantel tests with 1,000 permutations to assess statistical significance of the correlations (Hobson *et al.* 2013). We also tested for seasonal changes within the summer months by constructing aggregated networks for each study month (May-September) across all years and carrying out the same comparison procedure described above.

While the aggregation of several years of data allows for more precise estimates of contact probabilities, it also presents the potential for increasing the density (i.e. number of edges) in our simulated networks relative to the empirical annual contact patterns. Overestimating the density of contact networks can lead to overestimation of disease spread in epidemiological simulations (Risau-Gusman 2011). We carry out a simulation study to confirm that simulations based on the aggregated network do not result in higher density networks that would be expected for a single year of associations. For each year, we simulate associations for each dyad from a binomial distribution, using the observed annual dyadic sampling effort (D_{ij} in eq. 1) as the sample size and the aggregated SRI value as the probability of success. The expected mean annual density is then calculated from these simulated networks. We carry out this procedure 10,000 times to build a distribution of mean densities for our simulations, which is then compared to the mean density of the observed annual networks. If aggregation results in increased density, the observed mean density would be significantly lower than the simulated mean densities.

SRI networks were constructed in R (R Core Team 2017) using the asnipe package (Farine 2018) and custom code, and the vegan package was used to conduct Mantel tests (Oksanen *et al.* 2018).

Network metrics

To evaluate the precision of our social network, we estimated the correlation between our measured association indices and the underlying association probabilities. We first calculate the coefficient of variation (CV) of our observed SRI values, and then estimate the CV of the underlying association probabilities (S) via maximum likelihood, assuming the underlying associations follow a beta distribution. The ratio of S to the observed CV is an estimate of the portion of variance in SRI values that is accounted for by the variance in association probabilities, rather than sampling variance, and therefore approximates the correlation between true and observed association indices. Correlations greater than 0.4 are generally considered to indicate useful representations of the underlying social structure (Whitehead 2008). Parameter fitting was performed in R, using the VGAM package for beta-binomial likelihood calculation (Yee 2018).

We measure the extent to which individuals formed subgroups by performing community detection on the contact network. We use a walktrap community detection algorithm implemented in the igraph R package to detect communities (Csardi & Nepusz 2006). The modularity of the community division found by this algorithm is a network-level measure of how strongly individuals associate within rather than across social clusters.

Temporal independence of respiratory contacts

A key assumption of our disease transmission model (see below) is that the probability of a dyad coming into respiratory contact on a given day is constant, and therefore independent of contacts in previous days. Biologically, this would indicate that contacts dissolve and reform within a single day according to constant contact probabilities, leading to temporal independence of associations.

We test this assumption by calculating the lagged association rate (LAR) across several time-lags in our dataset. The LAR at time-lag τ estimates the probability that a dyad associated in a given day will also be associating τ days later. Most analyses of LAR analyze extremely large values of τ (i.e. over 1,000 days) in order to investigate the long-term temporal structure of associations. However, as we are interested in transmission dynamics over considerably shorter timescales (see below), we only investigate LARs for values of τ from 1 to 20 days.

Whitehead (1995) suggests comparing LARs to null association rates that represent the expected patterns if individuals associated randomly. As our model does not assume random mixing, but rather temporal independence, we use an alternative null association rate that approximates the expected LAR if associations dissolve and reform between each sampling period with a constant probability of association for each dyad. Let a_{ij} be the probability of an association between individuals i and j in each sampling period (approximated by SRI_{ij}). The probability that i and j associate twice in any two sampling periods, given independence, is then a_{ij}^2. The expected LAR across all time-lags under temporal independence (LAR_{null}) is then:

$$\mathrm{LAR}_{null} = \frac{\sum_i \sum_j a_{ij}^2}{\sum_i \sum_j a_{ij}} \qquad (2)$$

We calculated 95% confidence intervals for LARs at each τ using jackknife resampling (Whitehead 1995). LAR_{null} represents our null hypothesis of temporal independence, and we rejected this null hypothesis at

a given τ if the 95% confidence interval of the LAR at τ did not include LAR_{null}. All temporal analyses were performed using custom R code available in the supplementary material.

Disease outbreak model

We simulate the spread of CeMV using a stochastic individual-based susceptible-infected-removed (SIR) model over the killer whale respiratory contact network. Note that in SIR models, there is no difference between dead and recovered, immune individuals; they are removed from the population and cannot become infected again or spread the pathogen to others. While this framework is potentially overly simplistic for some pathogens, recovery from CeMV confers life-long immunity and the virus has no carrier state, meeting the basic assumptions of an SIR model (Van Bressem *et al.* 2014).

The model simulates a situation in which an interaction with a CeMV infected individual of another species (e.g. Pacific white-sided dolphin, humpback whale, harbor porpoise) leads to the introduction of the disease to the SRKW population via a single seed individual. Interspecific interactions are rarely observed, and therefore we assume no further interspecific transmission after the initial introduction. As CeMV has not been detected in this population in over 40 years of observations, all non-infected individuals start as susceptible. Each time-step in the model represents a single day. We therefore model the probability that an infected individual *j* transmits the disease to a susceptible individual *i* at time *t* (λ_{tij}) as the joint probability that *i* and *j* come into contact on that day and that a given contact effectively transmits the disease. As the fine-scale transmission dynamics of CeMV have not been resolved, we make the simplifying assumption that for each day a susceptible individual is exposed to an infected individual, there is a constant probability of transmission. We further simplify the model by assuming that daily contacts are independent of one another. We use our estimated SRI values to approximate daily contact probabilities, and so

$$\lambda_{tij} = \beta \cdot \mathrm{SRI}_{ij} \cdot I_{tj} \quad (3)$$

where β is the transmission coefficient, representing the per-contact probability of transmission, and I_{tj} is an indicator variable that takes the value of 1 if *j* is infected at time *t*, and 0 otherwise. The probability that susceptible individual *i* will become infected during timestep *t* (T_{ti}) is then

$$T_{ti} = 1 - \prod_j \left(1 - \lambda_{tij}\right) \quad (4)$$

346 The probability that individuals already infected at the beginning of timestep *t* will be removed by
347 timestep *t*+1 is denoted by α (mean infectious period = $1/\alpha$). Individuals that become infected during *t*
348 cannot infect others or be removed until timestep *t*+1. The model run is terminated when there are no
349 infected individuals left, or until the time limit is reached. We limit the number of daily time-steps to 150,
350 as our dataset represents association patterns during a five-month period of the year. We do not include
351 non-pathogen induced baseline mortality in the model, as mortality rates over a single 5-month period
352 would be too low to have a significant impact on model predictions. The disease simulation model was
353 coded in R and is available in the supplementary materials.

354

355 *Model parameters and output*

356 The outcome of our model is influenced by the removal probability α, and the transmission coefficient β.
357 We therefore sought to estimate values of these parameters that most closely resemble those of previous
358 CeMV outbreaks in wild odontocetes. In the absence of data on CeMV outbreaks in killer whale
359 populations, we estimate the likely range of epidemic parameters of CeMV from previously published
360 epidemic modelling and social network studies of western Atlantic bottlenose dolphins. We note that
361 CeMV strains vary in their epidemiology, and that there are likely differences in recovery rates and
362 infectiousness between host species (Jo *et al.* 2018). The derived parameter values should therefore be
363 viewed as rough estimates based on the best available knowledge.

364 Morris *et al.* (2015) estimated a reproductive ratio for CeMV (the average number of secondary cases
365 expected from a single infected individual, *R*) of 2.58 during the peak of an epidemic (95% CI = 2.08-3.17)
366 and a removal rate of 0.12 (95% CI = 0.1-0.14). While the overall rate at which infected individuals infect
367 others was estimated in this analysis, this study did not estimate a per-contact transmission probability.

368 To estimate the per-contact transmission probability of CeMV during this previously observed epidemic,
369 we use a social network study carried out by Titcomb *et al.* (2015) on a subpopulation of western Atlantic
370 bottlenose dolphins in the Indian River Lagoon to estimate the mean strength $\langle s \rangle$ of association networks
371 in this population. This study is the only large-scale social network study we are aware of in this species
372 that uses the same daily sampling period as our analysis, and spatially overlaps the CeMV outbreak from
373 which the other epidemic parameters were derived. This study reports a mean weighted degree in the
374 dolphin social network of 1.88 (95% CI = 1.63-2.13). We note that this study defined associations over
375 broader spatial scales than our analysis (100 m) and HWI was used, rather than SRI. These factors are

likely to produce estimates of $\langle s \rangle$ larger than our methodology, potentially leading to an underestimation of the transmission coefficient for CeMV and making our estimates of CeMV spread conservative.

For each set of simulations, we generate a set of α, $\langle s \rangle$, R_0, and seed individuals via Latin hypercube sampling using the "lhs" R package (Carnell 2019). This sampling technique allows for a more efficient exploration of the entire parameter space than sampling each variable independently (Seaholm *et al.* 1988). Parameter values for α, $\langle s \rangle$, and R_0 were drawn from continuous uniform distributions with ranges equal to their reported 95% confidence intervals, while the seed individual is draw from a discrete uniform distribution on [1, N], where N is the total number of individuals in the network (Table 1). We then calculate β for each parameter set using a simple estimate of the reproductive ratio for epidemics on weighted graphs (Kamp *et al.* 2013):

$$R_0 = \frac{\beta \langle s \rangle}{\alpha} \quad (5)$$

which can be re-arranged to

$$\beta = \frac{R_0 \alpha}{\langle s \rangle} \quad (6)$$

Our baseline simulation to assess overall vulnerability of the network consisted of 100,000 model runs. We evaluate the outcome of the model first by calculating the probability that an outbreak results in an "unusual mortality event" (UME; Gulland & Hall 2007). We use a simple heuristic to define UMEs, and say a UME has occurred when a simulation results in predicted mortality at least 2x higher than the highest recorded annual mortality rate in this population, which was 8.24% in 2016. Therefore, our definition of a simulated UME was a simulation in which at least 16.47% of the population is predicted to die. While the mortality rate of CeMV infected cetaceans is not known, individuals infected with viruses of this family tend to exhibit mortality rates of 70% - 80% (Diallo *et al.* 2007). We therefore assume that mortality rates due to CeMV were 70% of the final outbreak size, and thus our threshold outbreak size for UMEs was 23.53% of the population infected. While we use this threshold in the rest of the text, our general results were robust to alterations to this heuristic. We also calculated the mean and standard deviation of the outbreak size (the proportion of the population infected) during runs in which UMEs occurred as a measure of predicted UME severity.

We also conducted a sensitivity analysis to determine which of our two parameters, α and β, was most influential on the outcome of our simulation. We did this by calculating partial Spearman rank correlation coefficients for the final outbreak sizes of our 100,000 model runs and their respective values of these

two parameters (Wu *et al.* 2013). Higher absolute values of these coefficients indicate a greater amount of variance in the outcome of the simulation being due to variance in the parameter of interest, controlling for other parameters.

Influence of social structure on disease outbreaks

We next sought to determine the extent to which the structure of SRKW social relationships shapes disease spread. We do this by performing simulations of disease outbreaks on two null models. The first is a mean-field null model, in which all contact probabilities between individuals are set to the mean contact probability in the observed network. This model simulates a population that associates entirely at random, and is therefore equivalent to traditional epidemic models that assume random mixing. The second null model is an edge randomization, in which observed edge weights are randomly shuffled between dyads. This retains the heterogeneity of social preferences, but removes the higher-order structure of the network. In both null models, the mean strength (i.e. an individual's average contacts per time step) from the observed network is retained.

We carry out the same simulation procedure outlined above on the null-model networks, and examine the influence of network structure on disease dynamics by comparing the UME probability and mean UME size between the observed network and the two null models.

Effectiveness of vaccination

We next investigated whether a prophylactic vaccination strategy would be effective in this population. We simulate the implementation of three potential vaccination strategies. The first is a random vaccination, in which *V* randomly chosen individuals are set as removed prior to the start of the simulated outbreak. The other two strategies are both based on individuals' centrality in the network. In many networks, targeting vaccinations towards individuals with high weighted degree is the most effective strategy to induce herd immunity (Rushmore *et al.* 2014), however in networks with community structure, targeting high betweenness individuals that bridge communities is sometimes more effective (Salathe & Jones 2010). We simulate scenarios in which individuals are targeted either based on their weighted degree or weighted betweenness. In both scenarios, the *V* individuals with the highest centrality are set as removed prior to the start of the simulation.

We evaluate vaccination effectiveness relative to a "conservative coverage threshold" (Rushmore *et al.* 2014). We therefore define an effective vaccination coverage when UMEs do not occur in 95% of simulations. We simulate values of V from 1 to 50 (coverage of 1%-70%), with 50,000 simulations for each value of V and each vaccination strategy. We stress that safely vaccinating 50 free-ranging killer whales is most likely an unrealistic management goal, even if a safe and effective CeMV vaccine is developed for this species. Nonetheless, we simulate these high values to better illustrate the degree to which vaccination may be effective in this population.

Results

Respiratory contact structure

The final respiratory contact network contained a total of 72 individuals sighted over the course of 314 days of observation. All individuals were photographed on at least 30 different days throughout the study period, with a median of 82 days per individual. Estimation of social differentiation and subsequent comparison to the observed CV suggested a highly differentiated social structure and a good correlation between our observed network and the true underlying association probabilities (S = 1.50, r = 0.70).

All pairs of yearly networks were significantly positively correlated (range of r values= 0.41-0.58, all $p <$ 0.001), as were monthly networks (range of r values = 0.38-0.56, all $p < 0.001$). We therefore conclude that there is no evidence for significant changes in the patterns of social relationships within the summer months during our study period, nor was there evidence that social structure shifted significantly across the 5 years of the study. The mean density of annual networks was not different from the expected density given aggregated SRI values and sampling effort (Supp. Figure 1).

The aggregated SRKW respiratory contact network formed a single, highly connected component (Figure 1b). Over 70% of dyads had a non-zero contact probability during the study period. Non-zero edge weights ranged from 0.005 to 0.62, with the mean contact probability over all dyads being 0.03 (median = 0.01, IQR = 0.03).

In agreement with previous studies (Parsons *et al.* 2009; Ellis *et al.* 2017), the network was distinctly modular (Q = 0.52) and was divided into six social clusters. All but one cluster contained members of a single pod, the exception being J pod's cluster, which contained individual L87, an adult male that has frequently changed social affiliation since his mother's death in 2005 and has travelled with J pod since

2010 (Center for Whale Research 2018). L pod showed the most significant sub-pod structure, with three identified social clusters. In contrast, J pod formed a single, large cluster (Figure 1).

Analysis of lagged association rates showed that the temporal patterns of association in the observed data are largely similar to the expected patterns under temporal independence, given the observed association preferences. While the LAR is typically slightly above the expected LAR, jackknifed 95% confidence intervals overlap LAR_{null} (Supp. Figure 2). We conclude that our model's assumption of temporal independence is unlikely to significantly bias the results of our simulations.

Simulated disease outbreaks

As expected, the outcome of the baseline simulation showed distinct bimodality; the disease either failed to spread far beyond the initially infected individual, or most of the population became infected (Figure 2). The network was extremely susceptible to simulated CeMV outbreaks. The majority of simulations resulted in unusual mortality events (UME probability = 0.69). When UMEs occurred, the disease typically infected around 90% of the population (mean UME size = 0.89, SD = 0.09).

Sensitivity analysis using partial correlation coefficients suggested that the outcome of our model was more sensitive to variation in the per-contact transmission rate than the recovery rate. The partial rank correlation between outbreak size and transmission rate was 0.33, while the correlation with removal rate was -0.18. This is not surprising, as our values of the removal rate were based on the results of explicit epidemic modelling, while our estimates of the transmission rate were derived from a combination of previously reported epidemic parameters and social network metrics. The uncertainty in our estimates of the transmission rate therefore incorporate the uncertainty in recovery rate, basic reproductive number, and contact rates. While our range of recovery rates was 0.1 to 0.14, our final values of the transmission rate ranged from 0.1 to 0.27. This result highlights the need for further studies into the transmission dynamics of CeMV to inform modelling and management efforts. We note, however, that our estimates for the per-contact transmission rate of CeMV are highly conservative compared to the known transmission rates of other morbilliviruses (e.g. the 90% transmission rate found in measles; Hamborsky *et al.* 2015).

Influence of social structure on disease outbreaks

Comparison of results of simulations on the observed network to the two null models revealed that the structuring of contacts in the observed network provided limited protection from disease outbreaks (Figure 2). While UME probability was larger in the null models, the changes in UME probability were small (mean-field UME probability = 0.74; edge-randomized UME probability = 0.72). Similarly, the size of UMEs was slightly larger in both null models (mean-field: mean = 0.95, SD = 0.05; edge-randomized: mean = 0.93, SD = 0.06). In terms of number of individuals infected during UMEs, these differences amount to an average increase of 3 individuals in the edge-randomized model, and 5 individuals in the mean-field model. While these results suggest that both the strength and patterning of social preferences may lead to measurable reductions in epidemic probability and size, they also clearly demonstrate that these effects are likely not significant from the perspective of conservation planning in this population.

Effectiveness of vaccinations

Our network measures used to design vaccination strategies, weighted degree and betweenness, were not strongly correlated (Spearman's r = 0.24), indicating that there would be significant differences between vaccination strategies based on these measures. Both targeted vaccination strategies performed better than the random vaccination strategy at reducing the probability of outbreaks, and both targeted strategies performed similarly to one another. However, the differences in conservative coverage thresholds were modest. Given random vaccination, 45 individuals (62.5% coverage) were required to reduce UME probability below 0.05, compared to 40 individuals (55.6% coverage) in the betweenness strategy and 42 individuals (58.3% coverage) in the weighted degree strategy.

Discussion

In this study, we assessed the vulnerability of a critically endangered killer whale population to outbreaks of an infectious disease that has previously been identified as a potential hazard. In our analysis, designed to replicate the observed properties of cetacean morbillivirus, most simulations resulted in outbreaks that would likely result in unusual mortality events, and in these cases nearly the entirety of the population became infected. Our results further suggest that the social structure of this population offers only limited protection from disease outbreaks, and that vaccination programmes, even with relatively high coverage and ideal targeting of individuals, are unlikely to efficiently reduce the risk of outbreaks. Given its fragile state, it is unlikely that this population would recover from the sudden increase in mortality that would

result from a majority of the population becoming infected with CeMV. While this model was specifically parameterized to simulate the spread of CeMV, the general vulnerability suggested by this analysis is likely to be applicable to other highly infectious pathogens that can be spread via aerosols.

Theoretical models and comparative studies suggest that subgrouping in social networks reduces the risk of disease spread (Griffin & Nunn 2012; Sah et al. 2018). Our findings generally support this result, with the important caveat that the protection provided seems unlikely to be significant in a conservation context for this population. This agrees with recent simulation experiments suggesting that disease spread is only significantly inhibited at extreme modularity values, and that network fragmentation may be more important than modularity (Sah *et al.* 2017). We suggest that this lack of significant protection is due to the sheer density of connections in the killer whale network; while there were clear preferences for associating within clusters, associations across clusters were still common. In addition, modular structures are predicted to be most effective at trapping disease with low transmissibility (Sah *et al.* 2018). Social structure may therefore be less effective at trapping pathogens such as morbilliviruses, which are highly transmissible.

Both the distribution of contact probabilities and the degree of subgrouping had small but measurable effects on the outcomes of simulated epidemics. The effect of edge weight variance may partially be driven by the density of non-zero edges, as all individuals had the opportunity to interact in the mean-field model, while the edge-randomization maintained the portion of edges from the original network, although overall interaction rates were the same between the two models. In most cases, both the portion of non-zero edges and variance in edge weights are the result of social preferences in association networks (Whitehead 2008). Therefore, our findings suggest that both the intensity of social preference and the patterning of relationships may be determinants of disease spread on animal social networks. However, our study also demonstrates that small populations with strong social preferences and clear divisions between social units may still be highly vulnerable to the emergence of novel pathogens.

It is important to note that factors not included in the model, such as potential changes in social behavior after infection (e.g. Lopes *et al.* 2016; Stroeymeyt *et al.* 2018), the duration of daily social contacts, transitivity effects in the daily contacts, the potential for continued interspecies transmission, and variation in epidemic parameters, are likely to influence the actual outcome of CeMV outbreaks in this population. Our analysis draws particular attention to current uncertainty about the per-contact transmission rate of CeMV. We suggest that future empirical work address these knowledge gaps to better inform management efforts. Regardless, the results of our model are concerning, and suggest that the

possibility of widespread disease outbreaks and their potential impact on SRKW vital rates should be accounted for in future population assessments.

Our results demonstrate that it is difficult to induce effective herd immunity in the SRKW population by partial vaccination of the population, even when vaccinations are ideally targeted based on network centrality. At least 40 vaccinations (> 50% of the network) were required to reduce UME probability below 0.05, even with network-informed vaccination strategies. Modularity in contact structures is thought to generally make targeted vaccination more effective (Salathe & Jones 2010), however the multilevel nature of resident killer whale society complicates this; since family groups typically move together, there are no single individuals responsible for the majority of the spread between modules that can be targeted for vaccination. The logistical challenges of vaccinating and monitoring individuals at sea and the potential stress these activities may cause the animals likely make the prospect of wide-scale vaccinations impractical, as well as potentially unethical.

As individualized treatment is unlikely to be efficient, we suggest that management of potential disease outbreaks is likely best addressed by increasing the overall health of the population. Since the 1990s, the SRKW population has declined from nearly one hundred individuals to 73 at the time of writing. The most severe pressure contributing to this ongoing decline is reduced availability of prey (Lacy *et al.* 2017). As a result of consistently low food availability, visibly poor body condition is widespread in this population (Fearnbach *et al.* 2018), as is hormonal evidence of nutritional stress (Ayres *et al.* 2012). Poor nutrition may increase this population's vulnerability to CeMV and other pathogens (Aguilar & Raga 1993). While inbreeding and PCB concentration are also of concern due to their link to CeMV outbreaks (Aguilar & Borrell 1994; Valsecchi *et al.* 2003), these hazards are less readily addressed by conservation efforts. Therefore, in line with previous recommendations, we suggest that management actions designed to increase the abundance of Chinook salmon available to the SRKW are critical to mitigating the potential impact of epizootics in this population.

Our analysis highlights the importance of applying modelling techniques in conservation planning, while also highlighting the limitations of targeted vaccination as a disease management strategy. As conservation interventions are always limited by both resources (Bottrill *et al.* 2008) and potential negative impacts on individual animals (e.g. Woodroffe 2001), maximizing the payoff of management actions is crucial. Individualized medical interventions in general, and vaccinations in particular, are increasingly central to a number of conservation efforts. Previous work has demonstrated that modelling techniques can often inform low-impact, effective, and efficient vaccination programs in endangered

584 wildlife populations, particularly in primarily solitary species (Robinson *et al.* 2018) and in group-living
585 species with well-defined territories (Haydon *et al.* 2006). Our analysis suggests that such actions may be
586 less effective in highly social, group-living populations with frequent social contact between subgroups,
587 even when these groups are well defined. These social structures may also be generally vulnerable to
588 disease outbreaks, despite their apparent modularity. Such social structures are prevalent in several taxa
589 of conservation concern, including cetaceans, elephants, and primates (Grueter *et al.* 2012). We
590 recommend that similar simulation studies be implemented when evaluating infectious disease risk and
591 management strategies in these systems.

592

593 **References**

594 Aguilar, A., & Borrell, A. (1994). Abnormally high polychlorinated biphenyl levels in striped dolphins
595 (Stenella coeruleoalba) affected by the 1990-1992 Mediterranean epizootic. *The Science of the*
596 *Total Environment*, *154*(2–3), 237–247. https://doi.org/10.1016/0048-9697(94)90091-4

597 Aguilar, A., & Raga, J. A. (1993). The Striped Dolphin Epizootic in the Mediterranean Sea. *Ambio*, *22*(8),
598 524–528. https://doi.org/10.1111/1467-9752.12272

599 Alfonso, C. L., Amarasinghe, G. K., Banyai, K., et al. (2016) Taxonomy of the order *Mononegavirales*:
600 update 2016. *Archives of Virology, 161*(8), 2351-2360. https://doi.org/10.1007/s00705-016-2880-1

601 Allen L. J. S. (2008). An Introduction to Stochastic Epidemic Models. In: *Mathematical Epidemiology.*
602 *Lecture Notes in Mathematics 1945*. Brauer F., van den Driessche, P. & Wu, J. (eds). Springer,
603 Berlin, Heidelberg.

604 Ayres, K. L., Booth, R. K., Hempelmann, J. A., Koski, K. L., Emmons, C. K., Baird, R. W., Balcomb-Bartok, K.,
605 Hansen, M. B., Ford, M. J., & Wasser, S. K. (2012). Distinguishing the impacts of inadequate prey
606 and vessel traffic on an endangered killer whale (Orcinus orca) population. *PLoS ONE*, *7*(6).
607 https://doi.org/10.1371/journal.pone.0036842

608 Batley, K. C., Attard, C. R. M., Castillo, J. S., Zanardo, N., Kemper, C. M., Beheregaray, L. B., & Möller, L.
609 M. (2018). Genome-wide association study of an unusual dolphin mortality event reveals candidate

genes for susceptibility and resistance to cetacean morbillivirus, (August), 1–15. https://doi.org/10.1111/eva.12747

Bigg, M. A., Olesiuk, P. F., Ellis, G. M., Ford, J. K. B., & Balcomb, K. C. (1990). Social organization and genealogy of resident killer whales (*Orcinus orca*) in the coastal waters of British Columbia and Washington State. In P. Hammond, S. Mizroch, & G. Donovan (Eds.), *Individual Recognition of Cetaceans: Use of Photo-Identification and Other Techniques to Estimate Population Parameters* (pp. 383–405).

Bukreyev, A., Calisher, C. H., Dolnik, O., Domier, L. L., Du, R., Collins, P. L., … Kuhn, J. H. (2016). Taxonomy of the order *Mononegavirales*: update 2016, 2351–2360. https://doi.org/10.1007/s00705-016-2880-1

Cairns, S. J. & Schwager, S. J. (1987) A comparison of association indices. *Animal Behaviour* 35, 151-169

Carne, C., Semple, S., Morrogh-Bernard, H., Zuberbühler, K., & Lehmann, J. (2014). The risk of disease to great apes: Simulating disease spread in orang-utan (pongo pygmaeus wurmbii) and chimpanzee (pan troglodytes schweinfurthii) association networks. *PLoS ONE*, *9*(4). https://doi.org/10.1371/journal.pone.0095039

Carnell, R. (2019) lhs: Latin Hypercube Samples. R package version 1.0.1. https://CRAN.R-project.org/package=lhs

Center for Whale Research (2018). *Southern Resident Killer Whale ID Guide.* Center for Whale Research, Friday Harbor, WA, USA

Csardi, G., & Nepusz, T. (2006). The igraph software package for complex network research, InterJournal, Complex Systems 1695. http://igraph.org

Craft, M. E., & Caillaud, D. (2011). Network models: An underused tool in wildlife epidemiology? *Interdisciplinary Perspectives on Infectious Diseases*, *2011*. https://doi.org/10.1155/2011/676949

Craft, M. E. (2015). Infectious disease transmission and contact networks in wildlife and livestock. *Philosophical Transactions of the Royal Society B: Biological Sciences*, *370*(1669), 20140107–20140107. https://doi.org/10.1098/rstb.2014.0107

636 Cross, P. C., Lloyd-smith, J. O., Bowers, J. A., Hay, C. T., Getz, W. M., Annales, S., … Getz, W. M. (2004).
637 Integrating association data and disease dynamics in a social ungulate : bovine tuberculosis in
638 African buffalo in Kruger National Park. *Finnish Zoological and Botanical Publishing Board*, *41*(6),
639 879–892.

640 Daszak, P., Cunningham, A. A., & Hyatt, A. D. (2000) Emerging Infectious Diseases of Wildlife – Threats to
641 Biodiversity and Human Health. *Science, 287*(5452), 443-449.

642 Di Guardo, G., Marruchella, G., Agrimi, U., & Kennedy, S. (2005). Morbillivirus infections in aquatic
643 mammals: A brief overview. *Journal of Veterinary Medicine Series A: Physiology Pathology Clinical*
644 *Medicine*, *52*(2), 88–93. https://doi.org/10.1111/j.1439-0442.2005.00693.x

645 Ellis, S., Franks, D. W., Giles, D., Balcomb, K. C., Weiss, M. N., Cant, M. A., Nattrass, S., & Croft, D. P.
646 (2017). Mortality risk and social network position in resident killer whales: sex differences and the
647 importance of resource abundance. *Proceedings of the Royal Society B: Biological Sciences*,
648 *284*(1865).

649 Farine, D. R. (2018). asnipe: Animal Social Network Inference and Permutations for Ecologists. R package
650 version 1.1.8. https://CRAN.R-project.org/package=asnipe

651 Fearnbach, H., Durban, J., Ellifrit, D., & Balcomb, K. (2018). Using aerial photogrammetry to detect
652 changes in body condition of endangered southern resident killer whales. *Endangered Species*
653 *Research*, *35*, 175–180. https://doi.org/10.3354/esr00883

654 Ford, J. K. B., Ellis, G. M., Olesiuk, P. F., & Balcomb, K. C. (2010). Linking killer whale survival and prey
655 abundance: food limitation in the oceans' apex predator? *Biology Letters*, *6*(1), 139–142.
656 https://doi.org/10.1098/rsbl.2009.0468

657 Ford, M. J., Parsons, K. M., Ward, E. J., Hempelmann, J. A., Emmons, C. K., Hanson, B. M., Balcomb, K. C.,
658 & Park, L. K. (2018). Inbreeding in an endangered killer whale population. *Animal Conservation*
659 *21*(5), 423-432. https://doi.org/10.1111/acv.12413

Foster, E. A., Franks, D. W., Morrell, L. J., Balcomb, K. C., Parsons, K. M., van Ginneken, A., & Croft, D. P. (2012). Social network correlates of food availability in an endangered population of killer whales, Orcinus orca. *Animal Behaviour*, *83*, 731–736. https://doi.org/10.1016/j.anbehav.2011.12.021

Gaydos, J. K., Balcomb, K. C., Osborne, R. W., & Dierauf, L. (2004). Evaluating potential infectious disease threats for southern resident killer whales, *Orcinus orca*: A model for endangered species. *Biological Conservation*, *117*(3), 253–262. https://doi.org/10.1016/j.biocon.2003.07.004

Godfrey, S. S. (2013). Networks and the ecology of parasite transmission: A framework for wildlife parasitology. *International Journal for Parasitology: Parasites and Wildlife*, *2*(1), 235–245. https://doi.org/10.1016/j.ijppaw.2013.09.001

Griffin, R. H., & Nunn, C. L. (2012). Community structure and the spread of infectious disease in primate social networks. *Evolutionary Ecology*, *26*(4), 779–800. https://doi.org/10.1007/s10682-011-9526-2

Grueter, C. C., Matsuda, I., Zhang, P., and Zinner, D. (2012) Multilevel societies in primates and other mammals: Introduction to the special issue. *International Journal of Primatology, 33*(5), 993-1001. 10.1007/s10764-012-9614-3

Guimarães, P. R., De Menezes, M. A., Baird, R. W., Lusseau, D., Guimarães, P., & Dos Reis, S. F. (2007). Vulnerability of a killer whale social network to disease outbreaks. *Physical Review E - Statistical, Nonlinear, and Soft Matter Physics*, *76*(4), 42901. https://doi.org/10.1103/PhysRevE.76.042901

Gulland, F. M. D., & Hall, A. J. (2007). Is Marine Mammal Health Deteriorating? Trends in the Global Reporting of Marine Mammal Disease. *EcoHealth, 4*(2), 135–150. https://doi.org/10.1007/s10393-007-0097-1

Hamborsky, J., Kroger, A., & Wolfe, C. (2015). Epidemiology and prevention of vaccine-preventable diseases. United States: U.S. Dept. of Health & Human Services, Centers for Disease Control and Prevention.

Haydon, D. T., Randall, D. A., Matthews, L., Knobel, D. L., Tallents, L. A., Gravenor, M. B., Williams, S. D., Pollinger, J. P., Cleaveland, S., Woolhouse, M. E. J., Sillero-Zubiri, C., Marino, J., Macdonald, D. W., & Laurenson, M. K. (2006). Low-coverage vaccination strategies for the conservation of endangered species. *Nature, 443,* 692-695. https://doi.org/10.1038/nature05177

687 Hobson, E. A., Avery, M. L., & Wright, T. F. (2013). An analytical framework for quantifying and testing
688 patterns of temporal dynamics in social networks. *Animal Behaviour, 85*(1), 83-96.
689 https://doi.org/10.1016/j.anbehav.2012.10.010

690 Jo, W. K., Osterhaus, A. D. M. E., & Ludlow, M. (n.d.). ScienceDirect Transmission of morbilliviruses
691 within and among marine mammal species. *Current Opinion in Virology, 28,* 133–141.
692 https://doi.org/10.1016/j.coviro.2017.12.005

693 Kamp, C., Moslonka-Lefebvre, M., & Alizon, S. (2013). Epidemic Spread on Weighted Networks. *PLoS*
694 *Computational Biology*, *9*(12). https://doi.org/10.1371/journal.pcbi.1003352

695 Krahn, M. M., Hanson, M. B., Baird, R. W., Boyer, R. H., Burrows, D. G., Emmons, C. K., Ford, J. K. B.,
696 Jones, L. L., Noren, D. P., Ross, P. S., Schorr, G. S., & Collier, T. K. (2007). Persistent organic
697 pollutants and stable isotopes in biopsy samples (2004/2006) from Southern Resident killer whales.
698 *Marine Pollution Bulletin*, *54*(12), 1903–1911. https://doi.org/10.1016/j.marpolbul.2007.08.015

699 Krahn, M. M., Bradley Hanson, M., Schorr, G. S., Emmons, C. K., Burrows, D. G., Bolton, J. L., Baird, R. W.,
700 & Ylitalo, G. M. (2009). Effects of age, sex and reproductive status on persistent organic pollutant
701 concentrations in "Southern Resident" killer whales. *Marine Pollution Bulletin*, *58*(10), 1522–1529.
702 https://doi.org/10.1016/j.marpolbul.2009.05.014

703 Lacy, R. C., Williams, R., Ashe, E., Balcomb, K. C., Brent, L. J. N., Clark, C. W., Croft, D. P., Giles, D. A.,
704 MacDuffee, M., & Paquet, P. C. (2017). Evaluating anthropogenic threats to endangered killer
705 whales to inform effective recovery plans. *Scientific Reports*, *7*(1), 1–12.
706 https://doi.org/10.1038/s41598-017-14471-0

707 Lopes, P. C., Block, P. B, & Konig, B. (2016). Infection-induced behavioural changes reduce connectivity
708 and the potential for disease spread in wild mice contact networks. *Scientific Reports, 6*(1). 1-10.

709 Lusseau, D., Wilson, B., Hammond, P. S., Grellier, K., Durban, J. W., Parsons, K. M., Barton, T. R., &
710 Thompson, P. M. (2006). Quantifying the influence of sociality on population structure in
711 bottlenose dolphins. *Journal of Animal Ecology*, *75*(1), 14–24. https://doi.org/10.1111/j.1365-
712 2656.2005.01013.x

Lusseau, D., Whitehead, H., & Gero, S. (2008). Incorporating uncertainty into the study of animal social networks. Animal Behaviour, 75(5), 1809–1815. https://doi.org/10.1016/j.anbehav.2007.10.029

Morris, S. E., Zelner, J. L., Fauquier, D. A., Rowles, T. K., Rosel, P. E., Gulland, F., & Grenfell, B. T. (2015). Partially observed epidemics in wildlife hosts: Modelling an outbreak of dolphin morbillivirus in the northwestern Atlantic, June 2013-2014. *Journal of the Royal Society Interface*, *12*(112), DOI: 10.1098/rsif.2015.0676. https://doi.org/10.1098/rsif.2015.0676

NOAA (2018), *Updates on Southern Resident Killer Whales J50 and J35*. Retrieved from: https://www.westcoast.fisheries.noaa.gov/protected_species/marine_mammals/killer_whale/updates-j50-j35.html

Nunn, C. L., Jordan, F., Mc-Cabe, C. M., Verdolin, J. L., & Fewell, J. H. (2015). Infectious disease and group size: More than just a numbers game. *Philosophical Transactions of the Royal Society B: Biological Sciences*, *370*. https://doi.org/10.1098/rstb.2014.0111

Oksanen, J., Blanchet, F. G., Friendly, M., Kindt, R., Legendre, P., McGlinn, D., Minchin, P. R., O'Hara, R. B., Simpson, G. L., Solymos, P., Stevens, M. H. H., Szoecs, E., & Wagner, H. (2018). vegan: Community Ecology Package. R package version 2.4-6. https://CRAN.R-project.org/package=vegan

Parsons, K. M., Balcomb, K. C., Ford, J. K. B., & Durban, J. W. (2009). The social dynamics of southern resident killer whales and conservation implications for this endangered population. *Animal Behaviour*, *77*(4), 963–971. https://doi.org/10.1016/j.anbehav.2009.01.018

Pedersen, A. B., Jones, K. E., Nunn, C. L., & Altizer, S. (2007). Infectious Diseases and Extinction Risk in Wild Mammals. *Conservation Biology, 21*(5), 1269-1279.

R Core Team (2017). R: A language and environment for statistical computing. R Foundation for Statistical Computing, Vienna, Austria. URL https://www.R-project.org/

Raverty, S. A., Rhodes, L. D., Zabek, E., Eshghi, A., Cameron, C. E., Hanson, M. B., & Schroeder, J. P. (2017). Respiratory Microbiome of Endangered Southern Resident Killer Whales and Microbiota of Surrounding Sea Surface Microlayer in the Eastern North Pacific. *Scientific Reports*, *7*(1), 1–12. https://doi.org/10.1038/s41598-017-00457-5

739 Reynolds, J. J. H., Hirsch, B. T., Gehrt, S. D., & Craft, M. E. (2015). Raccoon contact networks predict
740 seasonal susceptibility to rabies outbreaks and limitations of vaccination. *Journal of Animal*
741 *Ecology*, *84*(6), 1720–1731. https://doi.org/10.1111/1365-2656.12422

742 Risau-Gusman, S. (2011) Influence of network dynamics on the spread of sexually transmitted diseases.
743 *Journal of the Royal Society Interface, 9.* http://doi.org/10.1098/rsif.2011.0445

744 Robbins M. M., Gray M., Fawcett K. A., Nutter F. B., Uwingeli P., Mburanumwe, I., Kagoda, E., Basobose,
745 A., Stoinski, T. S., Cranfield, M. R., Byamukama, J., Spelman, L. H., Robbins, A. M. (2011) Extreme
746 Conservation Leads to Recovery of the Virunga Mountain Gorillas. *PLOS ONE 6*(6).
747 e19788. https://doi.org/10.1371/journal.pone.0019788

748 Robinson, S. J., Barbieri, M. M., Murphy, S., Baker, J. D., Harting, A. L., Craft, M. E., & Littnan, C. L. (2018).
749 Model recommendations meet management reality: Implementation and evaluation of a network-
750 informed vaccination effort for endangered Hawaiian monk seals. *Proceedings of the Royal Society*
751 *B: Biological Sciences*, *285*(1870). https://doi.org/10.1098/rspb.2017.1899

752 Romano, V., Duboscq, J., Sarabian, C., Thomas, E., Sueur, C., & MacIntosh, A. J. J. (2016). Modeling
753 infection transmission in primate networks to predict centrality-based risk. *American Journal of*
754 *Primatology*, *78*(7), 767–779. https://doi.org/10.1002/ajp.22542

755 Rowles, T. K., Schwacke, L. S., Wells, R. S., Saliki, J. T., & Hansen, L. (2011). Evidence of susceptibility to
756 morbillivirus infection in cetaceans from the United States. *Marine Mammal Science*, *27*(1), 1–19.
757 https://doi.org/10.1111/j.1748-7692.2010.00393.x

758 Rozins, C., Silk, M. J., Croft, D. P., Delahay, R. J., Hodgson, D. J., McDonald, R. A., Weber, N., & Boots, M.
759 (2018). Social structure contains epidemics and regulates individual roles in disease transmission in
760 a group living mammal. *Ecology and Evolution,* in press. https://doi.org/10.1002/ece3.4664

761 Rushmore, J., Caillaud, D., Hall, R. J., Stumpf, R. M., Meyers, L. A., & Altizer, S. (2014). Network-based
762 vaccination improves prospects for disease control in wild chimpanzees. *Journal of the Royal*
763 *Society Interface*, *11*. https://doi.org/http://dx.doi.org/10.1098/rsif.2014.0349

764 Sah, P., Leu, S. T., Cross, P. C., Hudson, P. J., & Bansal, S. (2017). Unraveling the disease consequences
765 and mechanisms of modular structure in animal social networks. *Proceedings of the National*
766 *Academy of Sciences*, *114*(16), 4165–4170. https://doi.org/10.1073/pnas.1613616114

767 Sah, P., Mann, J., & Bansal, S. (2018). Disease implications of animal social network structure: A
768 synthesis across social systems. *Journal of Animal Ecology*, *87*(3), 546–558.
769 https://doi.org/10.1111/1365-2656.12786

770 Salathe, M., & Jones, J. H. (2010). Dynamics and Control of Diseases in Networks with Community
771 Structure. *PloS Computational Biology, 6*(4). e1000736.
772 https://doi.org/10.1371/journal.pcbi.1000736

773 Seaholm, S. K., Ackerman, E., & Wu, S. (1988). Latin hypercube sampling and the sensitivity analysis of a
774 Monte Carlo epidemic model. *International Journal of Bio-Medical Computing, 23*(1-2), 97-112.
775 https://doi.org/10.1016/0020-7101(88)90067-0

776 Silk, M. J., Croft, D. P., Delahay, R. J., Hodgson, D. J., Weber, N., Boots, M., & McDonald, R. A. (2017). The
777 application of statistical network models in disease research. *Methods in Ecology and Evolution*,
778 *8*(9), 1026–1041. https://doi.org/10.1111/2041-210X.12770

779 Springer, A., Kappeler, P. M., & Nunn, C. L. (2017). Dynamic vs. static social networks in models of
780 parasite transmission: predicting Cryptosporidium spread in wild lemurs. *Journal of Animal*
781 *Ecology*, *86*(3), 419–433. https://doi.org/10.1111/1365-2656.12617

782 Stroeymeyt, N., Grasse, A. V., Crespi, A., Mersch, D. P., Cremer, S., & Keller, L. (2018). Social network
783 plasticity decreases disease transmission in a eusocial insect. *Science, 362*(6417), 941-945.
784 https://doi.orf/10.1126/science.aat4793

785 Titcomb, E. M., O'Corry-Crowe, G., Hartel, E. F., & Mazzoil, M. S. (2015). Social communities and
786 spatiotemporal dynamics of association patterns in estuarine bottlenose dolphins. *Marine*
787 *Mammal Science*, *31*(4), 1314–1337. https://doi.org/10.1111/mms.12222

788 Valsecchi, E., Amos, W., Raga, J. A., Podestà, M., & Sherwin, W. (2004). The effects of inbreeding on
789 mortality during a morbillivirus outbreak in the Mediterranean striped dolphin (Stenella
790 coeruleoalba). *Animal Conservation*, *7*(2), 139–146. https://doi.org/10.1017/S1367943004001325

791 Van Bressem, M. F., Van Waerebeek, K., & Raga, J. A. (1999). A review of virus infections of cataceans
792 and the potential impact of morbilliviruses, poxviruses and papillomaviruses on host population
793 dynamics. *Diseases of Aquatic Organisms*, *38*(1), 53–65. https://doi.org/10.3354/dao038053

794 Van Bressem, M. F., Raga, J. A., Di Guardo, G., Jepson, P. D., Duignan, P. J., Siebert, U., Barrett, T., Santos,
795 M. C. O., Moreno, I. B., Siciliano, S., Aguilar, A., & Van Waerebeek, K. (2009). Emerging infectious
796 diseases in cetaceans worldwide and the possible role of environmental stressors. *Diseases of*
797 *Aquatic Organisms*, *86*, 143–157. https://doi.org/10.3354/dao02101

798 Van Bressem, M. F., Duignan, P. J., Banyard, A., Barbieri, M., Colegrove, K. M., De Guise, S., Di Guardo,
799 G., Dobson, A., Domingo, M., Fauquier, D., Fernandez, A., Goldstein, T., Grenfell, B., Groch, K. R.,
800 Gulland, F. Jensen, B. A., Jepson, P. D., Hall, A., Kuiken, T., Mazzariol, S. Morris, S. E., Nielsen, O.,
801 Raga, J. A., Rowles, T. K., Saliki, J., Sierra, E., Stephens, N., Stone, B., Tomo, Ikuko, Wang, J.,
802 Waltzek, T., & Wellehan, J. F. X. (2014). Cetacean Morbillivirus: Current Knowledge and Future
803 Directions. *Viruses*, *6*(12), 5145–5181. https://doi.org/10.3390/v6125145

804 Vaughan, K., Del Crew, J., Hermanson, G., Wloch, M. K., Riffenburgh, R. H., Smith, C. R., & Van Bonn, W.
805 G. (2007). A DNA vaccine against dolphin morbillivirus is immunogenic in bottlenose dolphins.
806 *Veterinary Immunology and Immunopathology*, *120*(3–4), 260–266.
807 https://doi.org/10.1016/j.vetimm.2007.06.036

808 Wang, W., Tang, M., Zhang, H., Gao, H., Do, Younghae, & Liu, Z. (2014) Epidemic spreading on complex
809 networks with general degree and weight distributions. *Physical Review E, 90*, 042803.
810 https://doi.org/10.1103/PhysRevE.90.042803

811 Wierucka, K., Verborgh, P., Meade, R., Colmant, L., Gauffier, P., Esteban, R., de Stephanis, R., & Canadas,
812 A. (2014). Effects of a morbillivirus epizootic on long-finned pilot whales *Globicephala melas* in
813 Spanish Mediterranean waters. *Marine Ecology Progress Series*, *502*1–10.
814 https://doi.org/10.3354/meps10769

Whitehead, H. (1995). Investigating structure and temporal scale in social organizations using identified individuals. *Behavioral Ecology*, *6*(2), 199–208.

Whitehead, H. (2008). *Analyzing Animal Societies: Quantitative Methods for Vertebrate Social Analysis*. University of Chicago Press.

Wu, J., Dhingra, R., Gambhir, M., & Remais, J. V. Sensitivity analysis of infectious disease models: methods, advances and their application. *Journal of the Royal Society Interface, 10*(86), 20121018 https://dx.doi.org/10.1098%2Frsif.2012.1018

Yange, Z., & Zhou, T. (2012). Epidemic Spreading in Weighted Networks: An Edge-Based Mean-Field Solution. *Physical Review E 85,* 056106. https://doi.org/10.1103/PhysRevE.85.056106

Yee, T. W. (2018). VGAM: Vector Generalized Linear and Additive Models. R package version 1.0-5. URL https://CRAN.R-project.org/package=VGAM

Figure 1. Respiratory contacts in the southern resident killer whale population. a) Example photographic sequence of a successive surfacing between two individuals (J42 and J16). Individual J42 is identifiable from her saddle patch in (i), and as J42 begins to submerge in (ii), individual J16 begins surfacing within one body length. In (iii), J16 is fully identifiable. b) Final respiratory contact network for the population from 2011 to 2015. Edge thickness corresponds to estimated daily probabilities of respiratory contact. Node colors indicate pod membership (blue = J, green = K, orange = L) and dotted lines indicate clusters found by walktrap community detection algorithm.

Figure 2. Distribution of disease outcomes in the observed network and two null models. Violin plots indicate the density of disease outcomes (in proportion of the population infected). Dotted line indicates our threshold for an unusual mortality event. Boxplots indicate quantiles for the runs in which the epidemic resulted in a UME.

Figure 3. Results of simulated vaccination strategies. Lines indicate UME probability for each vaccination strategy (solid = random, dashed = weighted degree, dotted = betweenness) under different levels of coverage. Red dotted line indicates our conservative vaccination target, at which UMEs are predicted to occur in less than 5% of cases.

860 Figure 1.

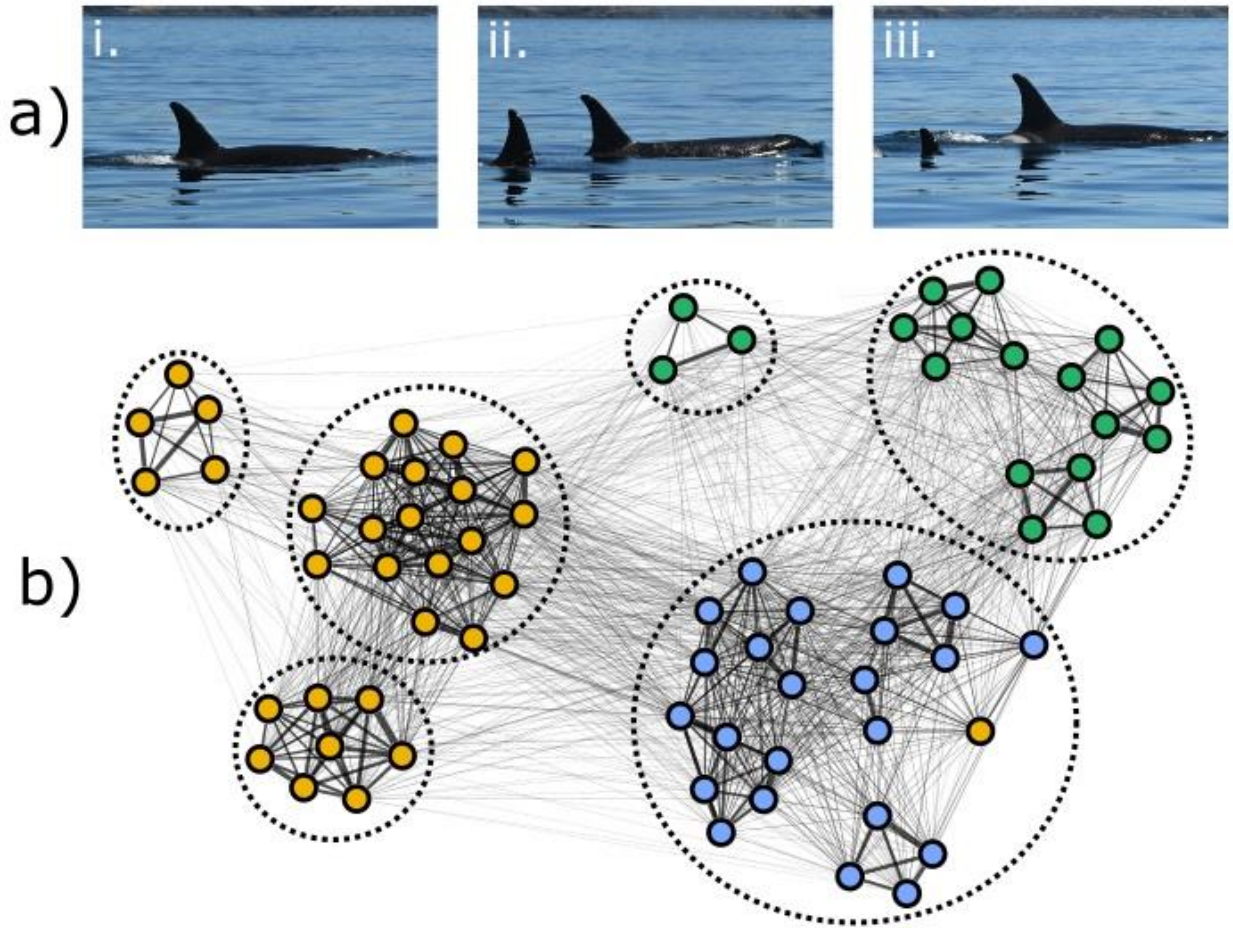

861

862

863

864

865

866

867

868

869 Figure 2.

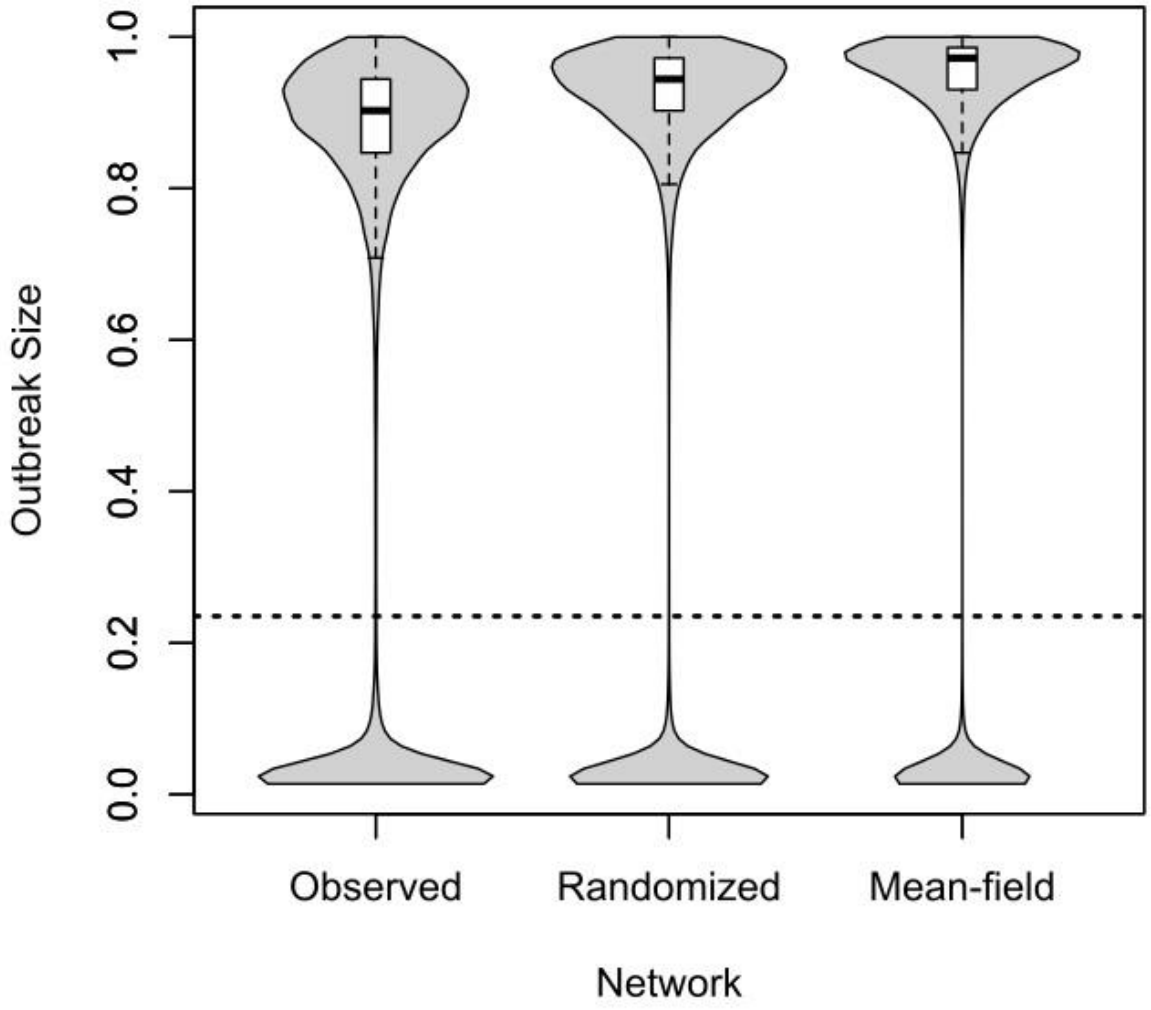

870

871

872

873

874

875 Figure 3.

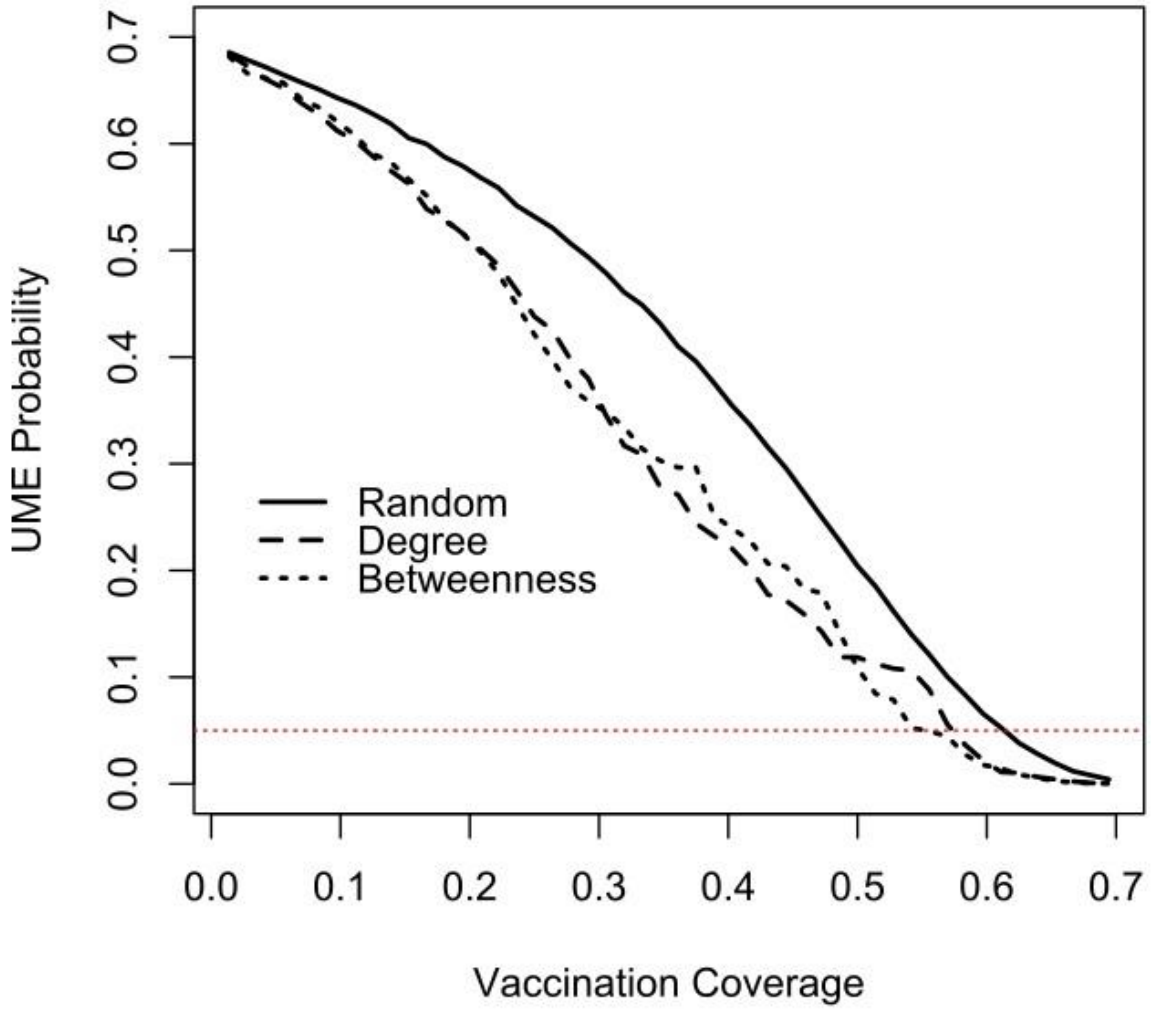

876

877

878

879

880 **Table 1.** Parameters and values used for disease simulations. All parameter ranges were derived from
881 studies of social interactions and CeMV epizootics in western Atlantic *T. truncatus.*

Parameter	Interpretation	Value	Source
α	Probability of removal per day	0.10 – 0.14	Morris *et al.* 2015
$1/\alpha$	Mean infectious period	7.14-10.00	Morris *et al.* 2015
R_0	Mean number of secondary cases per infected individual during an outbreak	2.08 – 3.17	Morris *et al.* 2015
$\langle s \rangle$	Mean number of contacts per individual per day	1.63 – 2.13	Titcomb *et al.* 2015
β	Per-contact transmission probability	$\frac{R_0 \alpha}{\langle s \rangle}$	Kamp *et al.* 2013

882
883
884
885
886
887
888
889
890
891
892
893
894
895

Supplementary Figures

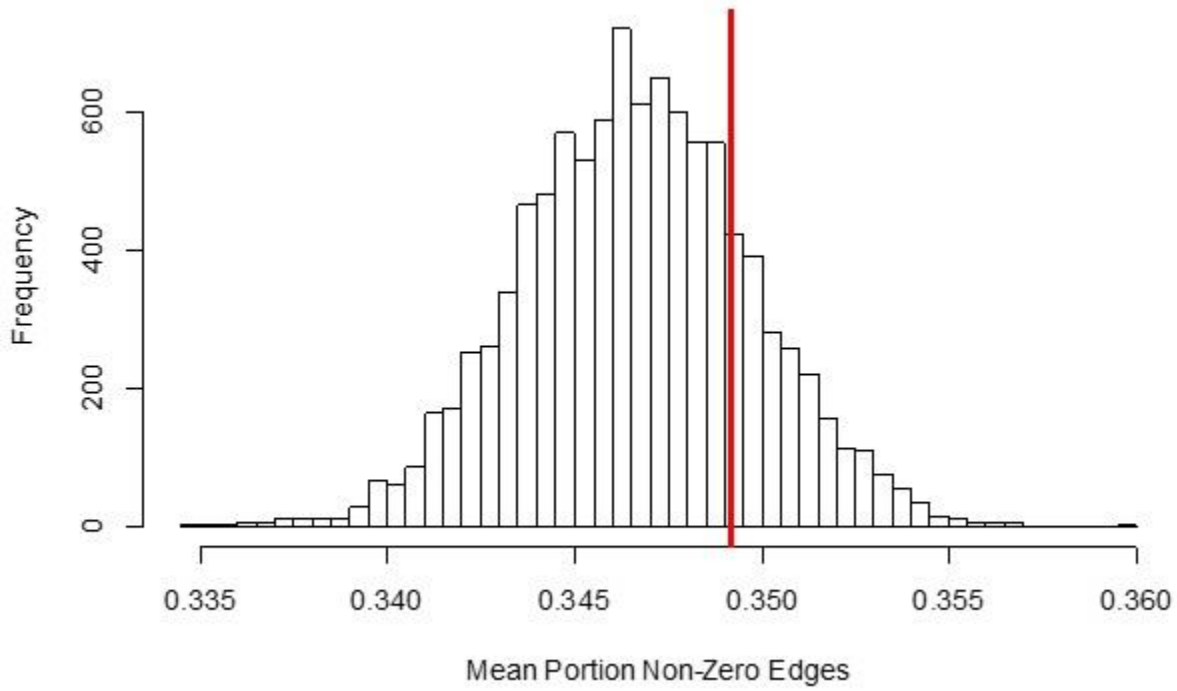

Supplementary Figure 1. Results of simulation comparing density of annual networks to aggregated network. Histogram represents the mean density of annual networks simulated from the aggregated contact probabilities and yearly dyadic sampling effort. Red line indicates the observed mean density of annual networks.

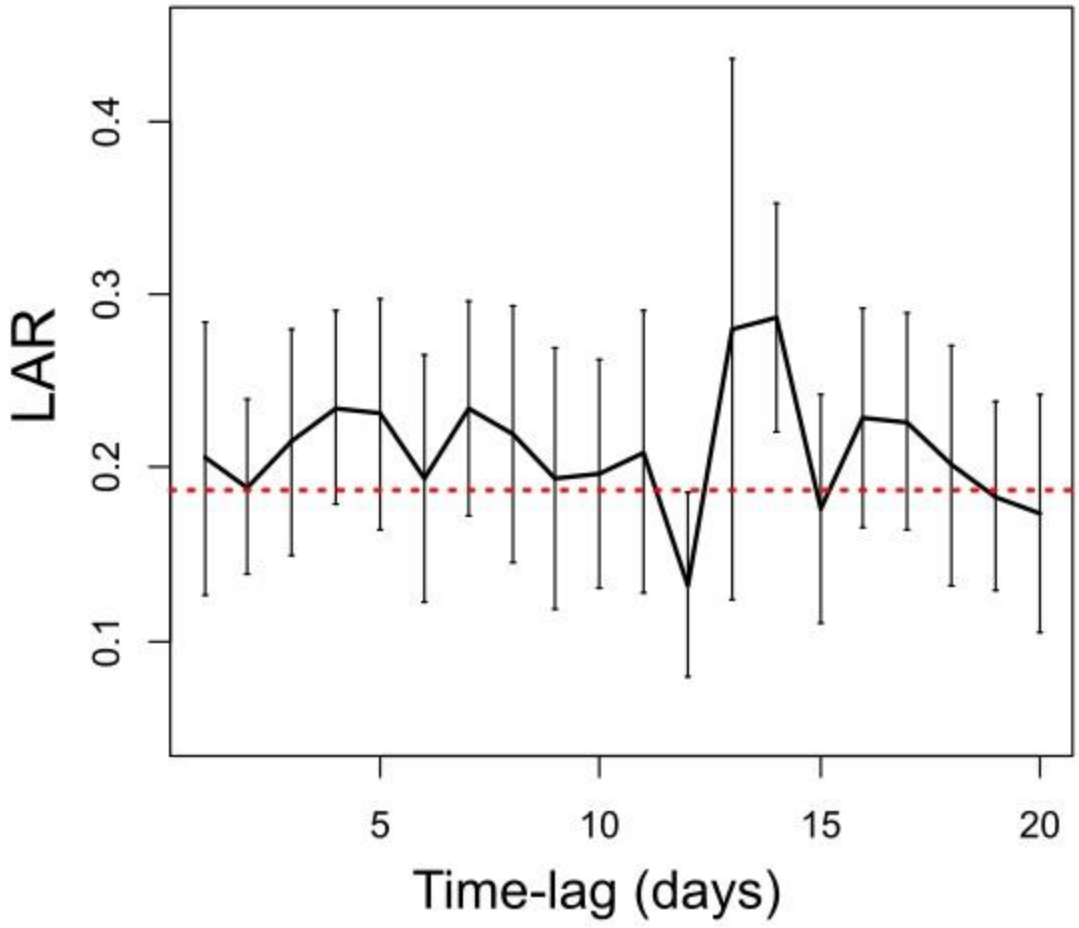

904

905 **Supplementary Figure 2.** Lagged association rates of respiratory contacts. Black line is the calculated LAR
906 at each daily time-lag, with error bars indicating jackknifed 95% confidence intervals. Dotted red line
907 indicates the expected LAR under temporal independence, given the observed association preferences
908 (as in equation 2).